Published in final edited form as:
Undersea Hyperb Med. 2013 ; 40(1): 23–31.

Diffusion tensor MRI of spinal decompression sickness

Elizabeth B. Hutchinson[1], **Aleksey S. Sobakin**[2,3], **Mary E. Meyerand**[4], **Marlowe Eldridge**[2,3], and **Peter Ferrazzano**[2,5]

[1]Department of Neurology, University of Wisconsin, UW Medical Foundation Centennial Building, Madison, Wisconsin USA

[2]Department of Pediatrics, University of Wisconsin, Clinical Science Center, Madison, Wisconsin USA

[3]Diving Physiology Research Laboratory, University of Wisconsin, Biotron, Madison, Wisconsin USA

[4]Department of Medical Physics, University of Wisconsin, Wisconsin Institutes Medical Research, Madison, Wisconsin USA

[5]Waisman Center for Intellectual and Developmental Disabilities, Madison, Wisconsin USA

Abstract

In order to develop more sensitive imaging tools for clinical use and basic research of spinal decompression sickness (DCS), we used diffusion tensor MRI (DTI) validated by histology to assess DCS-related tissue injury in sheep spinal cords. DTI is based on the measurement of water diffusion indices, including fractional anisotropy (FA) and mean diffusion (MD) to detect tissue microstructural abnormalities. In this study, we measured FA and MD in white and gray matter spinal cord regions in samples taken from sheep following hyperbaric exposure to 60–132 fsw and 0–180 minutes of oxygen pre-breathing treatment before rapid decompression. The main finding of the study was that decompression from >60 fsw resulted in reduced FA that was associated with cell death and disrupted tissue microstructure in spinal cord white matter tracts. Additionally, animals exposed to prolonged oxygen pre-breathing prior to decompression demonstrated reduced MD in spinal cord gray matter regions regardless of dive depth. To our knowledge, this is the first study to demonstrate the utility of DTI for the investigation of DCS-related injury and to define DTI biomarkers of spinal DCS.

INTRODUCTION

Neurologic decompression sickness (DCS) of the spinal cord is a diving-related injury resulting in acute and chronic sensory and motor impairments. Spinal DCS results when nitrogen bubbles form in the spinal cord vasculature and tissue in response to a rapid decrease in ambient pressure, which initiates a variety of pathological processes. Pathological correlates of spinal DCS include hemorrhage, axonal loss, myelin degeneration and inflammation [1].

The preferential involvement of spinal cord white matter remains to be fully understood, but likely involves direct damage due to autochthonous, or *in situ*, bubble formation. Nitrogen is highly soluble in the lipid-rich myelinated fibers of the spinal cord white matter, resulting in

Corresponding author: Dr. Peter Ferrazzano – ferrazzano@pediatrics.wisc.edu.

greater bubble formation in this region [2]. Consequently, the myelin sheath incurs global structural damage following DCS [3], including separation of myelin sheath layers [4].

Currently, diagnosis of spinal DCS is primarily made clinically. T2-weighted magnetic resonance imaging (MRI) has been used in suspected spinal DCS patients and has identified microhemorrhage or edema in the spinal cord [5]. However, many DCS patients suffer significant neurologic deficits despite normal T2 MRI scans, highlighting the inadequate sensitivity of currently used MRI techniques for diagnosis of spinal DCS [6]. Improved imaging tools are needed to better detect the primary pathologies of spinal DCS and for pre-clinical development of treatment strategies.

Diffusion tensor MRI (DTI) is an advanced MR imaging technique, which may be ideally suited for investigation of spinal DCS. DTI quantifies the direction and magnitude of the diffusion of water within tissue to infer microstructural properties [7,8]. The DTI metric of fractional anisotropy (FA) has been widely used in clinical and preclinical studies to report abnormalities in myelination and axonal integrity in the brain and spinal cord [9,10]. In contrast, the DTI metric mean diffusivity (MD) is very sensitive to cytotoxic edema and vascular changes that can occur following stroke [11]. Because both white matter damage and vascular compromise accompany spinal DCS, DTI is a promising tool for preclinical investigation of strategies to prevent or treat spinal DCS.

The primary objective of the present study was to identify and describe potential DTI markers of DCS-related spinal cord damage in a sheep model of hyperbaric exposure. Additionally, DTI was used to investigate the effect of variable lengths of oxygen prebreathing (O_2PB). The O_2PB intervention was designed as an alternative to lengthy staged decompression from large depths in emergency situations (*e.g.*, disabled submarine) [12,13] and has been shown to be effective for reducing incidence and severity of DCS [14–16].

We hypothesized that spinal DCS would manifest as reductions in the DTI parameter fractional anisotropy (FA) corresponding to altered myelination or axonal damage. Furthermore, it was expected that O_2PB would result in less spinal cord DTI abnormalities and improved clinical outcome.

METHODS

Hyperbaric exposure model of DCS in sheep

All animal procedures were performed in accordance with federal guidelines and under institutional oversight. Fourteen adult Suffolk ewes were acclimated to pressures of either 60 or 132 feet of sea water (fsw) in a dry hyperbaric chamber for 24 hours. Four control ewes were not exposed to the hyperbaric chamber. O_2PB intervention was administered to the dived sheep at 90% oxygen for 0, 15 or 180 minutes, followed by rapid (30 fsw/ minute) decompression to normal pressure (Table 1). Following decompression, sheep were monitored for clinical signs indicative of limb and respiratory DCS as described previously [15]. Briefly, limb DCS was rated by counting the number and duration of limb lifts in 10 minutes as follows:

- I – short lifts, resting behavior (< five lifts, duration < one second);
- II – full lifts (five-10 lifts, duration approximately one second);
- III – sustained lifts (> 10 lifts, duration > one second).

Respiratory DCS was graded as follows:

- Grade I – tachypnea, mild labored breathing;

- Grade II – restlessness, sporadic apnea, labored breathing;
- Grade III – severely labored breathing, neck extended, recumbent;
- Grade IV – collapse, stupor, death.

Spencer Bubble Score [17] was measured using precordial Doppler ultrasonography on surfacing and at one hour post-decompression as follows:

- 0 – complete lack of bubble signals;
- 1 – occasional bubble signal with the majority of cardiac periods free of bubbles;
- 2 – many, but less than half, of the cardiac periods contain bubble signals, singly or in groups;
- 3 – most cardiac periods contain showers of single-bubble signals, but not over-riding the cardiac motion signals;
- 4 – bubble signal detected continuously throughout systole and diastole of every cardiac period, and overriding normal cardiac signals.

In animals that died prior to completion of decompression or at time points after decompression, necropsy was performed; the spinal cord was harvested and immersion-fixed in paraformaldehyde (4%) within two hours of time of death. Necropsy and spinal cord harvest was similarly performed at six weeks post-decompression in animals that survived the immediate post-decompression period. For MRI, a segment of the thoracocervical spinal cord was rinsed in saline and encased in an airtight plastic sheet.

Imaging methods

Ex-vivo spinal cord imaging was performed using a 4.7T Agilent small animal MRI scanner. Three spinal cord samples and a saline reference phantom were imaged simultaneously during each 14-hour imaging session. The samples were placed so that images included a 46.5-mm length of each spinal cord in the region of the cervical enlargement. A 2D multislice spin echo pulse sequence was used for DTI with the following acquisition parameters:

- TE/TR = 22/2000 ms;
- nex = 4;
- FOV = 30×30 mm^2;
- slice thickness = 1.5mm;
- matrix = 192 × 192 reconstructed to 256 × 256;
- 31 slices;
- 3 non-weighted reference images and 30 diffusion weighted images (b~=1000 s/mm^2, non-colinear gradient directions).

Images were processed offline using a custom Matlab program to calculate the diffusion tensor and create index maps. A non-linear fitting algorithm was used to estimate the diffusion tensor [18] and the eigenvalues of the diffusion tensor (λ1, λ2 and λ3) were used to generate quantitative DTI maps of FA given by:

$$FA = \sqrt{\frac{(\lambda_1 - MD)^2 + (\lambda_2 - MD)^2 + (\lambda_3 - MD)^2}{2\left(\lambda_1^2 + \lambda_2^2 + \lambda_3^2\right)}}$$

and MD, given by MD = $(\lambda_1 + \lambda_2 + \lambda_3)/3$, as well axial diffusivity ($D_{||} = \lambda 1$) and radial diffusivity ($D_{\perp} = (\lambda_2 + \lambda_3)/2$), which are often reported to provide additional quantitative information about the shape of diffusion in the presence of FA abnormalities. FSL's FDT software was used to create directionally encoded color maps for visualization of directional information.

A semi-automated region of interest (ROI) based approach was used to generate binary masks for gray matter and white matter regions using FSL command line utilities and FSLview. FA thresholding was used to initially delineate white matter voxels, and the resulting masks were manually refined to yield three masks: dorsal columns, lateral columns and ventral columns.

Thresholding of the anatomical map from averaging all DTI volumes was used to delineate gray matter (GM), and the resulting masks were refined to yield three masks: dorsal horn, medial GM and ventral horn. These are shown in Figures 1A and 2A. Masks were applied to the image data to measure mean FA, MD, $D_{\perp}$ and $D_{||}$ within each ROI for each sample. MD, $D_{\perp}$ and $D_{||}$ values were normalized to a percentage of MD value in a saline reference phantom included in each scan.

Tissue processing and histology

Tissue from the center of the imaging volume was excised from the sample and sliced for histology using a freezing microtome to make 25-μm-thick sections. After immunostaining as described below, a Leica confocal microscope at 40x with FITC filters was used to acquire a 10-slice Z-series from each sample.

FluoroJade B staining of degrading neurons was performed as follows: Tissue sections were affixed to charge slides by floating in phosphate-buffered saline (PBS) and dried at 37°C. Slides were hydrated through an EtOH series (three minutes 100% EtOH, one minute 70% EtOH, one minute double-distilled H_20) and then transferred to a solution of 0.06% potassium permanganate for 15 minutes on a rotating platform at room temperature. Slides were rinsed for one minute in ddH_2O and then transferred to the FluoroJade solution (0.00005%) with 0.01% acetic acid for staining and gently shaken for 30 minutes at room temperature. Following staining, slides were rinsed three times for one minute each in ddH_2O, immersed in CitriSolve and then coverslipped with DPX.

Myelin basic protein staining was performed to evaluate for demyelination and axonal degradation as follows: Sections were stored in cryoprotection solution at −40°C until use, and a floating method was used to perform immunohistochemistry (IHC). First, sections were rinsed three times each with 0.01M PBS for five minutes. Sections were incubated in the blocking buffer of 10% goat serum for 30 minutes at 37°C and then incubated in the anti-mouse maltose binding protein (MBP) monoclonal antibody (Millipore, MAB387, 1:50) in antibody dilution buffer (2% goat serum) for one hour at 37°C followed by overnight incubation at 4°C. Sections were then rinsed three times with 0.01M PBS for 10 minutes and then incubated with the secondary antibody Alexa Fluor 488 goat anti-mouse (1:500, Molecular Probes, Eugene, Ore.) in antibody dilution buffer for one hour at 37°C. Sections were rinsed three times for five minutes and then mounted with Vecta-Shield fluorescence mounting medium.

Analysis and statistics

DTI measures were quantified within each ROI for each sample, and statistical analysis was performed using SPSS. To account for multiple comparisons across spinal cord regions, ANOVA was performed and Fisher's least significant difference post-test was applied to regions with a significant ANOVA. A p-value of < 0.05 was considered as significant. We

also report individual samples with DTI values found to be greater than two standard deviations away from the mean of the control values.

RESULTS

O_2PB is protective in decompression from 60 fsw

A summary of the post-dive clinical and bubble outcomes is given in Table 1. Animals without the O_2PB intervention survived < 60 minutes following decompression from 60 fsw. All animals in this group had a Doppler bubble score (DBS) ≥ 4, exhibited Grade IV respiratory DCS symptoms and Grade II limb DCS symptoms. Fifteen minutes of O_2PB improved survival to 75%, and reduced DBS and respiratory DCS scores. All animals exposed to 180 minutes of O_2PB prior to decompression from 60 fsw survived with dramatic reduction in limb and respiratory DCS symptoms noted in these animals despite DBS 2–3 in this group. The 180-minute O_2PB was not sufficient to protect against decompression from 132 fsw, as mortality was 100% in this group.

Decompression from 132 fsw results in reduced DTI FA values in spinal cord white matter regions

Decompression from 132 fsw resulted in a significant reduction in FA in the ventral column white matter (Figure 1, $p < 0.05$). Additionally, some samples in this group demonstrated reduced FA (>2SD from mean FA) in the dorsal columns as well. Interestingly, a single sample (Table 1, sample 4) in the 60-fsw / 15-minute O_2PB group was found to have reduced FA (>2SD from mean FA) in the dorsal columns. Additional analysis of radial diffusivity ($D_{\perp}$) and axial diffusivity ($D_{||}$) revealed no significant differences between groups. Importantly, no FA alterations were seen in the 60-fsw/ 180-minute O_2PB group.

180 minutes of O_2PB results in MD alterations in spinal gray matter

Decreases in gray matter MD were found compared to controls in animals exposed to 180 minutes of O_2PB (Figure 2). 180 minutes of O_2PB prior to decompression from 132 fsw resulted in a significant reduction in ventral horn MD (p<0.05). Similarly, 180 minutes of O_2PB prior decompression from 60fsw also resulted in significant ventral horn MD reductions. Interestingly, the two samples from each group with large reductions in MD in the ventral horn also demonstrated reduced MD (>2SD) in the medial gray matter. No alterations in MD were detected in the animals exposed to ≤ 15 minutes of O_2PB prior to decompression.

Decompression from 132 fsw results in cell death and alterations in myelination in spinal cord white matter

As shown in Figure 3, immunostaining in control samples demonstrated a dense network of axons with thick myelin sheaths, intense MBP staining, and no evidence of FluoroJade B-positive cells. Animals exposed to decompression from 132 fsw demonstrated numerous FluoroJade B-positive cells within the spinal cord white matter tracts (Figure 3e). Additionally, these samples exhibited decreased intensity of MBP staining, decreased axonal density and decreased diameter of myelinated fibers (Figure 3e′). Interestingly, the single sample from the 60-fsw/15-minute O_2PB group, which demonstrated white matter DTI abnormalities, also showed dramatic disruption of tissue architecture on FluoroJade B staining and MBP staining (Figures 3c, 3c′). The remaining samples demonstrated FluoroJade B staining and MBP staining similar to controls. No changes in FluoroJade B staining or MBP staining were found in gray matter regions.

DISCUSSION

In this study, we used diffusion tensor MRI to assess DCS-related spinal cord injury and the effect of O_2 pre-breathing prior to decompression. The main finding was that decompression from ≥ 60 fsw induced spinal cord white matter injury evidenced by reduced FA, cell death and disrupted tissue microstructure in spinal cord white matter tracts. It was also shown that animals exposed to the prolonged O_2PB treatment prior to decompression demonstrated reduced MD in spinal cord gray matter regions regardless of dive depth. To our knowledge, this is the first study to demonstrate the utility of DTI for the investigation of DCS-related injury and to define DTI biomarkers of spinal DCS.

Histopathologic correlates of DTI biomarkers of spinal cord DCS

DTI has been used clinically to assess white matter injury in a number of disease processes such as multiple sclerosis, traumatic brain injury, and ischemia (9). Both demyelination and loss of axons can be detected using DTI and manifests as reduced FA [10]. In this study, immunostaining of white matter regions with decreased FA revealed two profiles of white matter injury. Spinal cord white matter regions in the 132-fsw/ 180-minute O_2PB group demonstrated cell death and decreased myelination. Alterations in myelination at this acute time-point may be explained by direct damage to the myelin sheath by autochthonous bubble formation. Nitrogen is highly fat-soluble, resulting in increased bubble formation within the lipid-rich myelin sheath, especially on decompression from the extreme depths in this group. This evidence provides meaningful validation for the use of DTI as a proxy for white matter damage following DCS. The white matter FA reduction in the single sample from the 60-fsw/15-minute O_2PB group correlated with marked disruption of the tissue microarchitecture and decreased myelination. Taken together, this injury profile may be explained by extensive tissue damage due to a large load of autochthonous bubbles in this minimal O_2PB group. Alternatively, vasogenic edema formation due to venous congestion may account for the distortion and displacement of axon bundles seen in this specimen.

Alterations in mean diffusivity may represent cytotoxic edema formation as occurs acutely after ischemic injury [19]. At longer time scales, other mechanisms could underlie changes in MD, including vasogenic edema and inflammation, which are associated with increased MD or increased densities of cell bodies or axons, which are thought to reduce MD [9]. In this study, both groups of animals exposed to the 180-minute O_2PB demonstrated reduced MD in spinal cord gray matter. While we were unable to detect histopathologic correlates of these DTI findings using immuno-staining, the timing of these injuries gives some clue as to their cause. The early mortality in the group exposed to decompression from 132 fsw suggests that reduced MD in these animals is representative of ischemic injury. Large intravascular bubble formation on decompression from this extreme depth likely leads to ischemia and cytotoxic edema formation in spinal cord gray matter. Conversely, the reduced MD found in the 60-fsw/180-minute O_2PB group is unlikely to be secondary to ischemia, as these animals all survived for six weeks after decompression. MD deficits occur acutely after ischemic insult and normalize over the days following injury. The chronic MD reductions found in these animals may indicate a compensatory increase in neuronal density. Alternatively, oxidative stress due to the prolonged oxygen exposure at depth may result in chronic neuroinflammation and invasion of microglia in spinal gray matter.

Effect of dive depth and O_2PB on DTI measures of white matter injury

Tissue injury associated with spinal DCS is a complex series of overlapping and dynamic changes, including acute formation of autochthonous and vascular bubbles that can last hours and degenerative processes that may progress over the course of days and weeks following injury [20]. In this study, the greatest DTI abnormalities were detected in animals

exposed to the most severe dive paradigm (132 fsw) and from the one sheep that exhibited severe clinical signs of DCS following the less severe paradigm (60 fsw / 15 minutes O_2PB). The absence of DTI findings in the 60-fsw/0-minute O_2PB group suggests that the early mortality in these animals is due to respiratory DCS, without a significant contribution from spinal cord injury. DTI is a sensitive measure of white matter degeneration, and has been used clinically to monitor progressive white matter degeneration in human disorders such as cerebral ischemia, TBI and MS [21]. In this study, no white matter DTI changes were detected in the animals that survived six weeks following the dive, suggesting that O_2PB protects against chronic white matter injury in addition to improving survival.

LIMITATIONS AND FUTURE DIRECTIONS

The present study is an important first step toward the development of DTI for use in preclinical investigation of mechanisms, interventions and treatments of spinal DCS and the eventual translation for diagnostic and prognostic use in humans. However several limitations of this study should be discussed here and addressed in future work.

First, this study was designed as an initial investigation into the utility of DTI in identifying DCS pathology, and was not powered to detect differences in clinical outcome from O_2PB, so our ability to draw conclusions about the efficacy of O_2PB based on the results of this study is limited. We are similarly underpowered to comment on the sensitivity and specificity of DTI to detect histologic changes in a region specific manner.

Additionally, our results must be taken in light of the variable survival of the animals, and while every effort was made to perform necropsy as soon as possible after death of the animal, we cannot exclude postmortem bubble growth as a confounder of our *ex vivo* DTI findings. Inclusion of *in vivo* DTI in future studies using this sheep model of decompression sickness will help address these limitations.

In conclusion, our study suggests that DTI may be useful for assessment of spinal DCS-related tissue damage. In particular, we found that reduced white matter FA was associated with immunostaining evidence of injury in myelinated fibers likely due to autochthonous bubble formation. Additionally, this DTI marker suggested that O_2PB intervention is protective of the spinal cord at a dive depth of 60 fsw. This study highlights the potential for DTI in the preclinical development of effective interventions and treatments for spinal DCS. While recompression will remain the mainstay of treatment for spinal DCS, clinical use of DTI may ultimately prove useful in prognosis and in directing long-term treatment strategies for spinal DCS.

Acknowledgments

The authors thank Dandan Sun for assistance with histological and immunostaining methods, Ian Rowland for technical assistance with MRI sample preparation, and Doug Kintner for assistance with creation of figures. This work was supported by the NIH Clinical and Translational Science Award program NCATS 9U54TR000021 formerly NCRR 1UL1RR025011 (Ferrazzano), NIH P30 HD03352 (Waisman Center) and DOD, U.S. Navy (Eldridge).

References

1. Dick E, Broome J, Hayward I. Acute neurologic decompression illness in pigs: Lesions of the spinal cord and brain. Laboratory Animal Science. 1997 Feb; 47(1):50–7. [PubMed: 9051647]
2. Vernon, H. The solubility of air in fats, and its relation to caisson disease. Proceedings of the Royal Society of London. Series B, Containing Papers of a Biological Character; 1907. p. 366-71.
3. Bond JP, Kirschner DA. Spinal cord myelin is vulnerable to decompression. Molecular and Chemical Neuropathology. 1997; 30(3):273–88. [PubMed: 9165491]

4. Sykes J, Yaffe L. Light and electron microscopic alterations in spinal cord myelin sheaths after decompression sickness. Undersea & Hyperbaric Medicine. 1985; 12(3):251–8.
5. Gempp E, Blatteau JE, Stephant E, Pontier JM, Constantin P, Peny C. MRI findings and clinical outcome in 45 divers with spinal cord decompression sickness. Aviat Space Environ Med. 2008 Dec; 79(12):1112–6. [PubMed: 19070307]
6. Sparacia G, Banco A, Sparacia B, Midiri M, Brancatelli G, Accardi M, et al. Magnetic resonance findings in scuba diving-related spinal cord decompression sickness. Magnetic Resonance Materials in Physics, Biology and Medicine. 1997; 5(2):111–5.
7. Basser P, Mattiello J, LeBihan D. MR diffusion tensor spectroscopy and imaging. Biophys J. 1994; 66(1):259–67. [PubMed: 8130344]
8. Le Bihan D, Mangin JF, Poupon C, Clark CA, Pappata S, Molko N, et al. Diffusion tensor imaging: Concepts and applications. J Magn Reson Imaging. 2001 Apr; 13(4):534–46. [PubMed: 11276097]
9. Alexander AL, Lee JE, Lazar M, Field AS. Diffusion tensor imaging of the brain. Neurotherapeutics. 2007; 4(3):316–29. [PubMed: 17599699]
10. Budde MD, Kim JH, Liang HF, Schmidt RE, Russell JH, Cross AH, et al. Toward accurate diagnosis of white matter pathology using diffusion tensor imaging. Magn Reson Med. 2007 Apr; 57(4):688–95. [PubMed: 17390365]
11. Merino JG, Warach S. Imaging of acute stroke. Nat Rev Neurol. 2010 Oct; 6(10):560–71. [PubMed: 20842186]
12. Castagna O, Gempp E, Blatteau JE. Pre-dive normobaric oxygen reduces bubble formation in scuba divers. Eur J Appl Physiol. 2009; 106(2):167–72. [PubMed: 19219451]
13. Gennser M, Blogg SL. Oxygen or carbogen breathing before simulated submarine escape. J Appl Physiol. 2008 Jan; 104(1):50–6. [PubMed: 17975127]
14. Mahon RT, Dainer HM, Gibellato MG, Soutiere SE. Short oxygen prebreathe periods reduce or prevent severe decompression sickness in a 70-kg swine saturation model. J Appl Physiol. 2009 Apr; 106(4):1459–63. [PubMed: 19179650]
15. Sobakin A, Lehner C, Wilson M, Gendron-Fitzpatrick A, Sauder A, Eldridge M. Dysbaric osteonecrosis in UW sheep DISSUB trials after a 3-hour oxygen pre-breathe before dropout decompression. Undersea Hyperb Med. 2008; 35(4)
16. Butler B, Little T, Cogan V, Powell M. Hyperbaric oxygen pre-breathe modifies the outcome of decompression sickness. Undersea Hyperb Med. 2006; 33(6):407–17. [PubMed: 17274310]
17. Spencer MP. Decompression limits for compressed air determined by ultrasonically detected blood bubbles. J Appl Physiol. 1976 Feb; 40(2):229–35. [PubMed: 1249001]
18. Koay CG, Chang LC, Carew JD, Pierpaoli C, Basser PJ. A unifying theoretical and algorithmic framework for least squares methods of estimation in diffusion tensor imaging. Journal of Magnetic Resonance. 2006; 182(1):115–25. [PubMed: 16828568]
19. van Gelderen P, de Vleeschouwer MH, DesPres D, Pekar J, van Zijl PC, Moonen CT. Water diffusion and acute stroke. Magn Reson Med. 1994 Feb; 31(2):154–63. [PubMed: 8133751]
20. Francis, TJ.; Mitchell, SJ. Pathophysiology of decompression sickness. In: Bove, AA.; Davis, JC., editors. Bove and Davis' Diving Medicine. 4. Philidelphia: Saunders; 2004. p. 165-184.
21. Sundgren PC, Dong Q, Gomez-Hassan D, Mukherji SK, Maly P, Welsh R. Diffusion tensor imaging of the brain: Review of clinical applications. Neuroradiology. 2004 May; 46(5):339–50. [PubMed: 15103435]

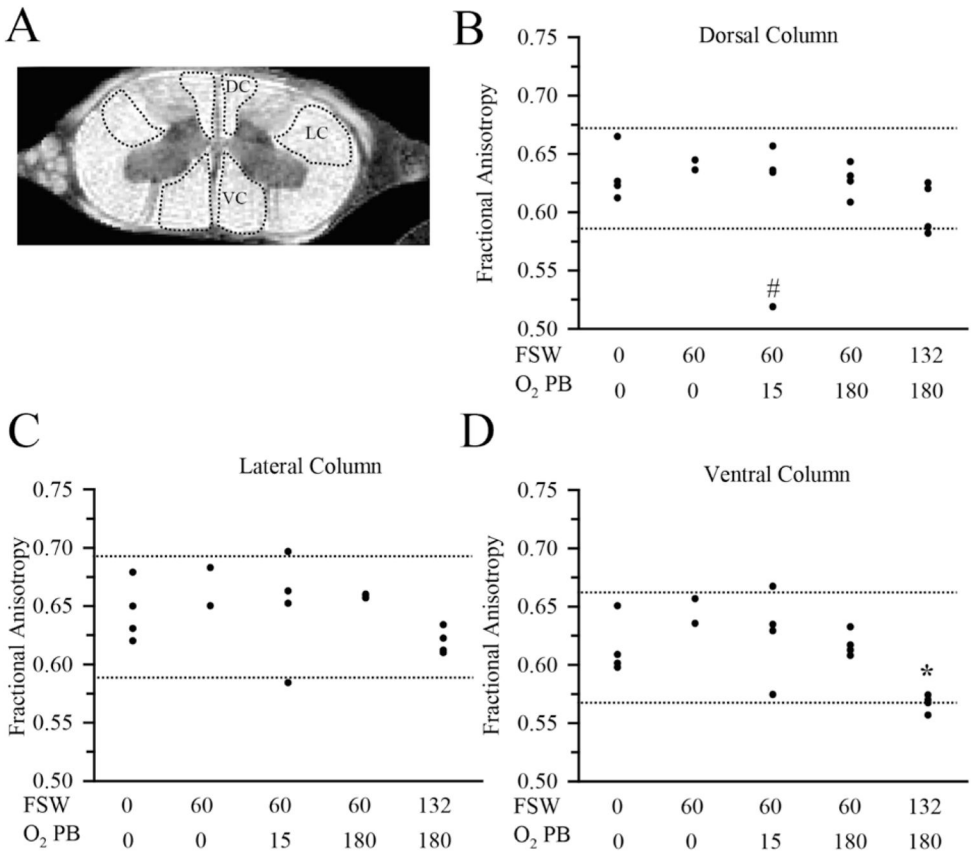

FIGURE 1. ROI masks, white matter

ROI masks are shown in A for three white matter regions: dorsal column (DC), lateral column (LC) and ventral column (VC). FA values are shown for each sample from the control and experimental groups for dorsal column (B), lateral column (C) and ventral column (D). Dashed lines indicate FA values corresponding to two standard deviations above or below the mean of control FA values. * denotes a significant (p<0.05) group difference from control values. # indicates animal 4 from Table 1.

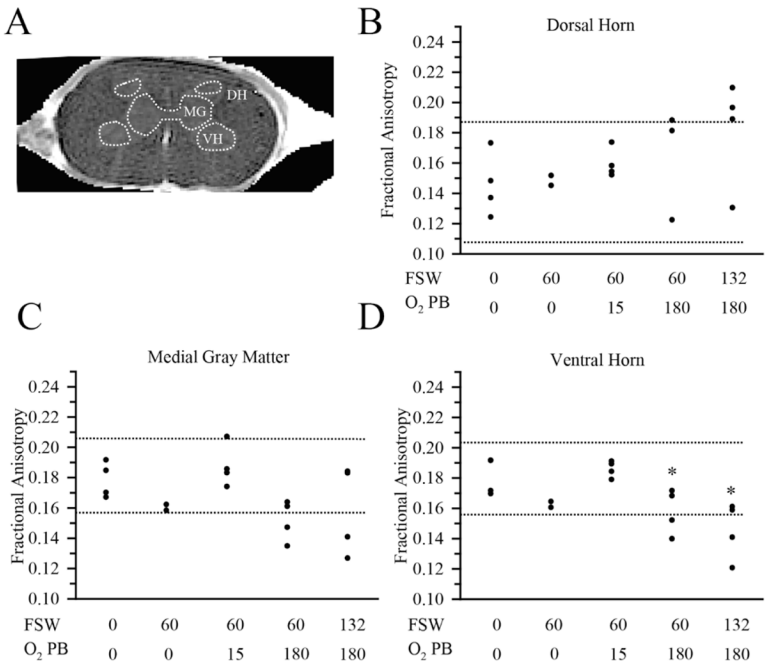

FIGURE 2. ROI masks, gray matter

ROI masks are shown in A for three gray matter regions: dorsal horn (DH), medial gray matter (MG) and ventral horn (VH). Normalized MD values are shown for each sample from the control and experimental groups dorsal horn (B), medial (C) and ventral horn (D). Dashed lines indicate values corresponding to two standard deviations above or below the mean of control values. * denotes a significant (p<0.05) group difference from control values.

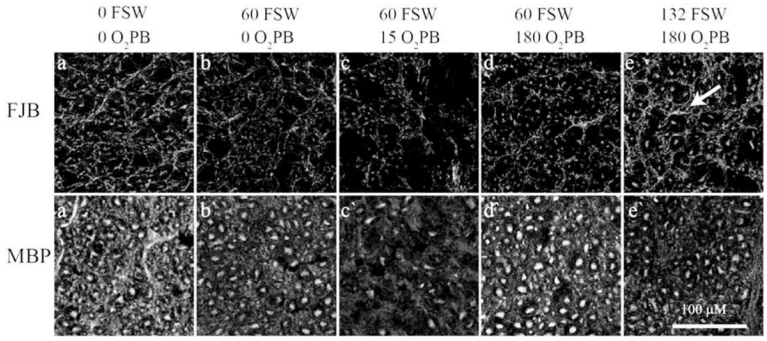

FIGURE 3. Fluorescence images

Fluorescence images are shown for histological staining for FluoroJade B (FJB, top row) and immunostaining for myelin basic protein (MBP, bottom row) in WM from a representative sample in each group as labeled. 60-fsw / 15-m O2PB images are from animal 4 (Table 1).

TABLE 1

Sample characteristics and clinical outcome data

Depth	O_2PB duration	No.	Survival outcomes (min)	Limb DCS rating	Respiratory DCS grade	Doppler bubble score	
						Surface	1 hour
60 fsw	0 min	1	56	II	IV	4	-
		2	34	-	IV	4+	-
60 fsw	15 min	3	survived	III	0	2	3+
		4	1230	III	III	4+	4+
		5	survived	III	I	2	3+
		6	survived	III	0	2-	4
60 fsw	180 min	7	survived	II	0	3+	4+
		8	survived	I	0	3	4
		9	survived	I	0	3	4+
		10	survived	I	0	2	4
132 fsw	180 min	11	8	-	IV	-	-
		12	75	-	IV	-	-
		13	0	-	-	-	-
		14	0	-	-	-	-

The four experimental groups were defined by depth of dive and length of O_2PB. The clinical outcome data includes survival duration (animals that survived for six-week duration of study are denoted by "survived" and animals that died prior to completion of decompression are denoted by "0"), limb DCS rate from least to most severe (I–III), respiratory DCS grade from least to most severe (I–IV) and doppler bubble score from least to most bubbles (0–4+) upon surfacing and one hour after surfacing. Clinical scores were unable to be assessed in some animals with early mortality.